Moving Hydrogen through the UK Gas Distribution Network

Michael Sargent [ID][a,*], Philip Sargent [ID][a]

[a]Cambridge Energy UK, 27 Greville Road, Cambridge CB1 3QJ, UK

Abstract

We state the appropriate thermodynamic and transport properties to use for the delivery of hydrogen through pre-existing natural gas distribution networks. We show that the flow is not as fully-turbulent as past work has assumed, that hydrogen makes the flow even less turbulent, and that the pipe friction calculation requires more careful treatment in this partially-turbulent regime.

We propose that the relevant final energy demand is the energy delivered as heated water. The different dew points of the flue gases from hydrogen versus natural gas combustion affect the boiler efficiency. This impacts the relative amount of hydrogen required to be delivered.

We find that to deliver the same amount of useful energy as hot water, hydrogen requires a gas velocity of $3.076\times$ and a pressure gradient that is $1.29\times$ higher. The compression power increase required to deliver hydrogen through the low pressure network can be up to $7.85\times$ that for natural gas, depending on the flow regime.

Keywords: Hydrogen, pipe-flow, friction factor, natural gas, condensing boiler, gas velocity.

1. Introduction

A possible future for the UK gas network is to reuse parts of it to distribute hydrogen instead of natural gas[1]. Two recent reports[2, 3] excellently summarise the current complex issues regarding replacing natural gas with hydrogen in the UK in political and techno-economic terms, however they do not cover the detailed flow characteristics of hydrogen in pipes.

In recent years it has become apparent that reusing parts of the low pressure distribution grid is a very different problem from re-using the intermediate pressure distribution grid or the transmission grid[4, 5].

While a high pressure transmission system for hydrogen may be required in the UK[6], this would largely be new construction built in parallel with the existing natural gas National Transmission System. However parts of the intermediate and low pressure distribution system would be repurposed from natural gas to carry hydrogen.

We have determined that there are no prior, sound, theory-based studies of the flow of hydrogen through pipes under the conditions typical of the last sections of the distribution network.

Therefore, these are the questions we want to answer:

1. Can the pipework supply enough hydrogen to match the energy demand of domestic housing?

2. What are the pressure and gas velocity differences?
3. How much extra energy would be required to deliver the hydrogen?

1.1. Bossel

The first attempt at this work was made by Bossel[7] but he considered pure methane, not natural gas, through a transmission pipe with assumed fully-turbulent flow. To date, Bossel is still used[8] as a basis flow calculations, even for situations outside his original assumptions, and full reassessment of his first-principles calculation is overdue.

In the distribution system we find that non-linear friction effects become significant and the flow is not fully-turbulent. Models which have used Bossel's number are inaccurate for distribution and may not be quite right for transmission either, quite apart from using the wrong gas.

1.2. Out of scope

Distributing hydrogen has other complexities that this paper does not address. These include: maintaining the required concentration when blended with natural gas[4], Joule-Thompson cooling and liquid dropout[9], compressor issues[10], compatibility with vehicle tanks[11], linepack and high- and intermediate pressure networks[12], and materials issues[3].

2. Standard gas and reference conditions

Public data on the exact composition of natural gas in the UK national transmission system is sparse. There are

---

*Corresponding author: Michael Sargent

Email addresses: `michael.sargent@cambridgeenergy.uk` (Michael Sargent [ID]), `philip.sargent@cambridgeenergy.uk` (Philip Sargent [ID])

URL: 0000-0001-9129-2990 (Michael Sargent [ID]), 0000-0002-0968-4467 (Philip Sargent [ID])

	[mol/mol]		[mol/mol]
CH_4	89.5514 %	iC_5	0.0344 %
C_2H_6	5.1196 %	$neoC_5$	0.0020 %
C_3H_8	1.3549 %	C_6	0.2377 %
nC_4	0.2162 %	CO_2	2.0743 %
iC_4	0.1269 %	N_2	0.9354 %
nC_5	0.3472 %		

Table 1: Composition of NG at Fordoun NTS on 20th Jan.2021.[13]

regulatory limits on certain properties of the gas, including the Wobbe number, density, and calorific value under defined conditions.

As a concrete example, this paper uses the composition of the gas taken directly from an 84 bar NTS transmission pipe at Fordoun (near Aberdeen) on 20 Jan.2021[13] as the composition of natural gas (NG).

This gas has 11 components: methane, ethane, propane, n-butane, iso-butane, n-pentane, iso-pentane, neo-pentane, hexane (including traces of higher hydrocarbons), carbon dioxide, and nitrogen. The Peng-Robinson equation of state can be used to calculate the average properties of this mixture[14]. The mixture has a molecular weight of 18.359 g/mol, a higher heating value of 940.813 kJ/mol and a density of 0.83556 kg/m^3 at 8°C.

The conditions of the gas in the distribution network that were used for these and all other material properties are representative of gas in the Service Line pipe entering a UK home during winter. The temperature of the gas in the distribution network is not significantly different from that of the surrounding ground, and the ground temperature at the depth of the distribution network will be about 8°C during the winter months on average[15]. The average pressure in the distribution network is taken to be 40 mbar above one atmosphere (1.05325 bar)[3, 16][1].

3. Delivering combustion energy through a pipe

In comparing the delivery of natural gas and hydrogen through a pipe system, the metric by which they must be evaluated is the delivery of the same heat to the consumer.

3.1. Molar Properties

When dealing with natural gas, quantities of the gas are often expressed either as mass, or volume at standard temperature and pressure. However as we are comparing different compressible gases (see Appendix B), both in the transport as well as the chemical reaction of combustion, we shall work in moles of gas. An ideal gas obeys the ideal gas law, equation (1).

---

[1]We do not consider deviations from these conditions for the purpose of calculating material parameters, as the deviations in conditions are not large enough to cause significant changes to the material parameters

$$P V_{ideal} = n R T \qquad (1)$$

where n is the number of moles of gas, R is the ideal gas constant (8.3145 J/mol·K), P is the absolute pressure, and T is the absolute temperature.

We account for non-ideality of the gases by using the compressibility factor, Z, which is the ratio of the actual volume to that of an ideal gas under the same conditions:

$$Z = \frac{V_{real}}{V_{ideal}} \qquad (2)$$

Z is related to the external conditions via the molar volume, the volume of one mole of gas, V_m, which is linearly proportional to Z by the conditions of the gas:

$$V_m = \frac{V_{real}}{n} = \frac{Z R T}{P} \qquad (3)$$

3.2. Energy delivered

For the flow of a fuel through a pipe, such as the distribution system which supplies natural gas to domestic homes, the energy supply may be calculated by equation (4).

$$Q = A v \frac{[\text{HHV}]}{V_m} \eta = A v [\text{HHV}] \frac{P}{Z R T} \eta \qquad (4)$$

Q, is the rate at which useful combustive energy is transferred along the pipe, in kJ/s. A is the cross section area of the supply pipe in m^2. v is the linear velocity of the gas in m/s, which is the parameter that may be controlled to modify the rate of energy transfer to account for differences between the two gases.

The important gas properties are the molar volume, V_m, in m^3/mol, and the Higher Heating Value, [HHV], also called the heat of combustion, in kJ/mol. Lastly, η is the efficiency of combustion reactions of the gases within domestic boiler systems.

To calculate the difference in gas velocity required for hydrogen compared to natural gas, equation (4) is calculated for each gas[2] for the same value of Q, and then the ratio of the two gives equation (5). We are considering the two gases in the same section of the distribution system, thus the pipe cross section area A and the temperature T, which should be equal to the ground temperature, are not included as they will be the same for both gases.

$$\left(\frac{v_{H_2}}{v_{NG}}\right) = \frac{\left(\frac{Z_{H_2}}{Z_{NG}}\right)}{\left(\frac{[\text{HHV}]_{H_2}}{[\text{HHV}]_{NG}}\right)\left(\frac{P_{av,H_2}}{P_{av,NG}}\right)\left(\frac{\eta_{H_2}}{\eta_{NG}}\right)} \qquad (5)$$

Equation (5) shows that there are four terms that affect how much more gas is needed when switching from natural gas to hydrogen, each given as a ratio:

---

[2] The thermophysical data used in the paper come from NIST[17] and also from the CoolProp project[18] which publishes the algorithms as open source code.

1. Compressibility factors
2. Higher heating values (by mole)
3. Pipeline pressures (average)
4. Boiler efficiencies

We will look at these ratios and compare the relative magnitudes of their effects on the overall velocity ratio. Note that as this form uses the molar HHV, the effect of density has been confined to the compressibility factor.

3.3. Compressibility factor

The compressibility factor, Z, of any gas is a quantitative measure of its non-ideal behaviour. The temperature dependence of Z for hydrogen, natural gas, and pure methane is shown in Figure 1. The dependence on pressure is very slight for the narrow pressure range present in the distribution system[19, 1].
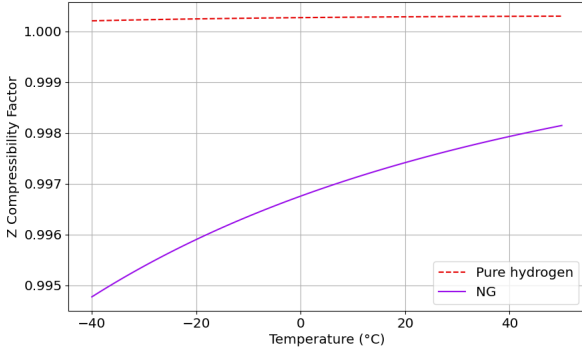

Figure 1: Plot of gas compressibility factors Z, showing the deviation from the ideal gas value of 1.0 calculated using the Peng-Robinson equation of state at 8°C[14]. The effect of 75 mbar pressure on Z is minute.

In the distribution pipework the compressibility factor of hydrogen is nearly constant at 1.0003 and the compressibility factor of natural gas is 0.997 at 8°C[14]. This means that the ratio of compressibility factors is $Z_{H_2}/Z_{NG} = 1.003$. This is a very small effect that is potentially within the uncertainty of other parameters in equation (5).

3.4. Higher Heating Values [HHV]

Of these four terms in Equation (5), the HHV of the gases is the simplest as it is a molecular property that does not depend on the conditions of the gas. All Higher Heating Value data are by convention referred to a standard temperature and pressure of 25°C and 1 atm, i.e. close to room temperature. The HHV is the energy of the reaction in which the fuel and oxygen start at 25°C and 1 atm, are combusted, and then the sensible and latent heat of the combustion products is recovered as they are brought back down to 25°C and all the water is condensed[20]. The HHV of natural gas and hydrogen are shown in Table 2.

A naive approximation to calculating the ratio of gas velocities may be made by assuming both gases to be close

	HHV [kJ/mol]
H$_2$	285.826
NG	940.813
ratio	0.304
reciprocal	3.292

Table 2: Higher Heating Values at 25°C and 1 atm.

to ideal, the pressures close to atmospheric, and the boiler efficiencies to be the same for hydrogen and natural gas. Under these assumptions, then the velocity ratio would be equal to the reciprocal of the HHV ratio as shown in Table 2, and the velocity of hydrogen required to supply the same quantity of heat would be $3.292 \times$ that of natural gas. Previous studies have published a value of 3.13 for this velocity ratio, because they did not use the correct values for natural gas[1, 7]. The major cause of this difference is the approximately 7% by mole of longer hydrocarbons in UK natural gas that raise the molar HHV significantly compared to pure methane (Table 1).

3.5. Average pressure

The average pressure in the distribution network will depend on the pressure drop in the delivery of the gas along the pipes, which in turn depends on the velocity of the gas. We are using the average pressure for natural gas as 40 mbar above atmospheric[16], but we require a value for hydrogen. This requires an iterative solution procedure which will be performed in Section 4.4, so for now we simply state the result, that the average pressure for hydrogen is 45.88 mbar above atmospheric. Therefore the ratio of average pressures is $P_{av,H_2}/P_{av,NG} = 1.0056$.
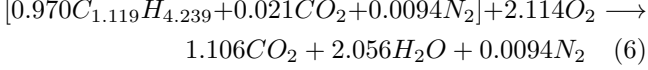
3.6. Boiler efficiency

The efficiency of a domestic boiler is highly dependent on the design and operation of each individual unit. Rather than attempt to quantify the diverse array of domestic boilers in use in the UK, we will instead look at how the *maximum possible efficiency* differs for hydrogen and natural gas, and assume that the operation relative to this maximum efficiency is comparable for the two fuels. This means we are not considering gas velocity or heat transfer within the heat exchanger section of the boiler. We categorise boilers into one of two operating modes:

- A non-condensing boiler vents the flue gas, the products of the combustion, with all of the water still in the gas phase.

- A condensing boiler attempts to recover latent heat by condensing some of the water vapour into liquid water.

The HHV is the absolute maximum energy that may be obtained from the fuel so the boiler efficiency η will be relative to the HHV[21]. Furthermore, as the fuel is not

burned in pure oxygen, there is sensible heat lost to heating up the nitrogen in the air. Also a boiler will typically operate with 15% excess air, to ensure complete combustion of the fuel[22]. Any heat which is not recovered by not condensing water vapour, and inlet and outlet gases not being at 25°C and 1 atm, is a reduction in efficiency[21].

$$[0.970C_{1.119}H_{4.239}+0.021CO_2+0.0094N_2]+2.114O_2 \longrightarrow$$
$$1.106CO_2 + 2.056H_2O + 0.0094N_2 \quad (6)$$

The overall combustion reaction of one mole of the UK natural gas is given by equation (6), and the HHV of this reaction is 940.813 kJ/mol[20]. The list of reagents (fuel and air) and products of the combustion are shown in table 3. All of the combustible hydrocarbons have been combined into one pseudo-component[18] (see Appendix B), with a mole-averaged heat capacity of 37.276 kJ/mol·K[17] and the air is approximated as a mixture of 20.95% oxygen and 79.05% nitrogen[3]

Species	Reagents [mol]	Products [mol]	Products [mol/mol]	C_p [J/mol·K]
C_nH_m	0.970			37.38
O_2	2.431	0.307	2.49%	36.28
N_2	9.181	9.181	73.99%	29.12
CO_2	0.021	1.140	8.94%	36.81
H_2O		2.119	16.61%	32.89 $_{(g)}$
				75.63 $_{(l)}$

Table 3: NG combustion reaction in 15% excess air, with pseudo-component $C_n H_m$ where n=1.119 and m=4.239, and heat capacity C_P values[17] at 8°C and 1 atm.

It can be seen that the flue gas from burning NG is rich in nitrogen (73.99%), with water as second highest fraction (16.61%). As water is the only condensable component in the flue gas[4], the dew point of the mixture is the temperature at which the equilibrium vapour pressure of water is equal to its partial pressure[24]. In this mixture, 16.61% mole fraction of water corresponds to a partial pressure of 0.1661 atm, which is the vapour pressure of water[24] at 56.4°C (see Appendix E). This means that a boiler must cool the flue gas below this temperature for any condensation to occur.

As the representative temperature for a condensing boiler, we choose to use the recommended return flow temperature for central heating water of 50°C[25]. As we are neglecting inefficiencies in heat transfer within the boiler, the return flow temperature is taken to be equal to the flue gas exit temperature[5] The equilibrium vapour pressure of

water at 50°C is 0.1218 atm, and the partial pressure of water vapour in the flue gas is reduced to this value when 16.6% of the water present in the vapour has condensed out of the gas phase, leaving 72.4% of the water still as vapour. Under these conditions, there are four contributions to the loss of efficiency.

First, latent heat is required to evaporate 72.4% of the 2.119 moles of water. The heat of vaporisation of water at 25°C is 43.99 kJ/mol, which means that the latent heat lost in the boiler is 77.83 kJ (per mole of NG).

Second, the natural gas in the distribution system is at 8°C, as mentioned in Section 2. Sensible heat is required to bring it to 25°C, which are the conditions of the reagents according to definition of HHV. Using the heat capacity values from Table 2, heating the gas up to these conditions requires 0.522 kJ (per mole of NG). The variation of heat capacities with temperature is neglected for all species, due to the narrow temperature range being considered.

Third, the air will be at a different temperature to the natural gas. We assert that the best air temperature to use is the mean temperature weighted by gas use, i.e. that temperature for which the amount of fuel burned in colder days matches that burned in warmer days. This is the mean temperature on a plot of daily fuel use against temperature on that day[6] and Terry and Galvin[27] model this as 5°C. Heating the air up to these conditions requires 6.77 kJ (per mole of NG).

Lastly, the flue gas and condensed water is heated from 25°C, the conditions according to the definition of HHV, to the exit temperature of 50°C. Heating the flue gas up to these conditions requires 9.40 kJ (per mole of NG).

In total, this tells us that of the 940.8 kJ of HHV energy released from the combustion of one mole of NG, 95.55 kJ is lost, which is a maximum efficiency of $\eta_{NG} = 89.95\%$ when the flue gas temperature is 50°C.

Now let us compare this to the combustion reaction for hydrogen, which is given by equation (7), and the HHV of this reaction is 285.8 kJ/mol. The list of reagents and products is shown in table 4.

$$H_2 + 0.5O_2 \longrightarrow H_2O \quad (7)$$
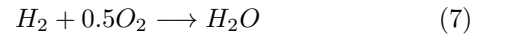
Comparing table 3 with table 4 we see that the flue gas from hydrogen combustion has nearly double the fraction of water than from combusting NG, 30.8% instead of 16.6%. This has the beneficial result that the partial pressure of water is higher, and thus that the dew point temperature is also higher at 70.0°C. Thus a pure-hydrogen condensing boiler does not need to run as cold to start recovering latent heat, and will recover more latent heat if operated at the same temperature.

---

[3]The weather-dependent humidity of the inlet air has an insignificant effect on the subsequent calculations, as does the small quantity of the pollutant NO_x produced in the combustion.

[4] Carbon dioxide may be neglected due to low solubility in water[23].

[5] The condensing temperature of the flue gas will not be the same as the water return temperature, as the heat exchanger is not

infinitely long. A temperature difference of up to 5°C may calculated from the efficiency values reported in[21, 26].

[6]Ideally for boiler efficiency calculations this would be on an hourly basis, not a daily basis.

Species	Reagents [mol]	Products [mol]	Products [mol/mol]	C_p [J/mol·K]
H_2	1			28.76
O_2	0.575	0.075	2.31%	29.34
N_2	2.170	2.170	66.87%	29.12
H_2O		1	30.82%	32.89 (g)
				75.63 (l)

Table 4: Hydrogen combustion reaction in 15% excess air, with heat capacity C_p[17] at 8°C and 1 atm.

For the same representative 50°C flue gas temperature, 68.87% of the water vapour will condense out of the gas phase.

Repeating the same calculations as for natural gas, the total sensible heat lost is 5.06 kJ/mol and the latent heat lost is 12.97 kJ/mol, both of which are per mole of hydrogen combusted. In total, this tells us that of the 285.8 kJ of HHV energy released from the combustion of one mole of hydrogen, 18.0 kJ is lost, which is a maximum efficiency of $\eta_{H_2} = 93.7\%$ when the flue gas temperature is 50°C.

We reason that a condensing boiler operating with a 50° flue gas temperature has a higher possible maximum efficiency when using hydrogen fuel than when using natural gas, as the higher dew point temperature means it is more easily able to recover heat by condensing water vapour out of the gas phase. Conversely if this heat is *not* recovered by condensation, such as by an imperfectly controlled boiler, then the efficiency *decreases* significantly.

These calculations[7] may be repeated for any specified flue gas exit temperature. If that is above the dew point then *all* of the latent heat of the water is lost. This data is plotted in Figure 2.
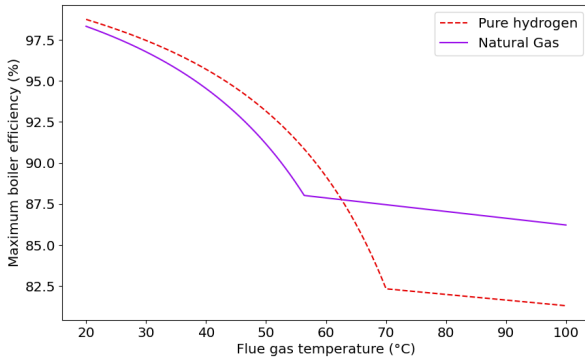

Figure 2: Maximum thermodynamic HHV efficiency of representative natural gas (blue) and hydrogen (red) combustion in 15% excess air as a function of the temperature to which the flue gas is cooled. The kink is at the temperature above which no condensation occurs.

[7] We have calculated dew points for 10 natural gas compositions, from Tokyo and the Netherlands to Algeria and the North Sea. The dew point temperatures range from 56.03 to 58.8°C[14].

It can be seen that the lines for hydrogen and NG in Figure 2 intersect at 63°C. For a flue gas temperatures below this value, the hydrogen combustion has a *higher* maximum possible efficiency. For flue gas temperatures above this value, the hydrogen combustion has a *lower* maximum possible efficiency. The gradient of the efficiency curve above the dew point temperature[8] represents the sensible heat loss by the heat capacity of the flue gas: much of this is required to heat the nitrogen in the inlet air.

For equation (5), we require a ratio of the two efficiencies. If we assume that all the existing boilers are condensing, and that all of them are perfectly adjusted with a flow temperature of 50°C, then the efficiency ratio would be $\eta_{H_2}/\eta_{NG} = 1.027$. This parameter is placed on the denominator of equation (5), and so because hydrogen boilers are more efficient, the velocity ratio will be decreased by accounting for boiler efficiencies.

However, it is not sensible to assume that all existing boilers operate this optimally. We have data on how many piped-gas boilers in the UK are condensing, but we would need to make an assumption as to how this would change after conversion to pure hydrogen boilers. Current regulations[28] are that all new boilers must be condensing, so the population boiler efficiency ratio will change substantially purely from this, without including the extra benefit from having a higher-efficiency fuel. In addition, it is highly doubtful that all current condensing boilers are correctly set with a return flow temperature of 50°C whereas it is more likely that more of the new hydrogen boilers would be configured correctly. Appendix C calculates that an appropriate overall efficiency multiplier using 2022 data would be $\eta_{H_2}/\eta_{NG} = 1.067$.

3.7. Velocity ratio

Combining all of terms that have been calculated for equation (5) gives us, from equation (8), a value of 3.076 for the ratio of the velocities of hydrogen to natural gas through the same pipes.

- The ratio of compressibilities is 1.003, which increases the required velocity of hydrogen.

- The ratio of HHVs is 0.304, indicating that hydrogen is produces significantly less energy when combusted than natural gas, on a molar basis.

- The ratio of average pressures is 1.0056. This value is determined iteratively from the velocity ratio in Section 4.4.

- The ratio of boiler efficiencies is 1.067, indicating that condensing boilers burning hydrogen combustion are more efficient than those burning natural gas.

[8]In some published versions of this boiler characteristic, if the line to the right of the dew point is horizontal, it means that those authors have not calculated the sensible heat loss.

$$\left(\frac{v_{H_2}}{v_{CH_4}}\right) = \frac{1.003}{0.304 \times 1.0056 \times 1.067} = \mathbf{3.076} \quad (8)$$

This velocity ratio is very close to the reciprocal of the molar HHV ratio. The compressibility ratio and average pressure ratio each contribute less than 1% change to the velocity ratio. The largest secondary effect is the efficiency of condensing boilers.

These are the values for the Fordoun natural gas. We have also run the same calculations with other gas mixtures and there is no substantive difference in the results (details are listed in the software [14]).

4. Flow though pipes

We need a way of comparing the flow of hydrogen with the flow of natural gas through a pipe. There is a wide choice of apparently useful equations[9] available in the gas industry, but almost none are correct for hydrogen and few describe the range of flow regimes we need to understand.

We need to take a more fundamental approach. At the low pressure and narrow pressure range present in the distribution grid, the incompressible fluid approximation is accurate[24], so we should use the Darcy-Weisbach equation for the pressure drop along a pipe:

$$\Delta p = f\left(\frac{L}{D}\right)\frac{1}{2}\rho v^2 \quad (9)$$

where L is the length of the pipe, D the diameter of the pipe, v is the mean velocity of the gas, ρ the density, and f the Darcy friction factor.

The Darcy friction factor is a dimensionless parameter that determines the resistance to flow. It depends on the type of flow, or regime, that the fluid experiences.

The different flow regimes are separated by the relative importance of inertial and viscous forces. The ratio of these two behaviours is the Reynolds number, Re, which also serves as a dimensionless form of the velocity:

$$Re = \left(\frac{\rho v D}{\mu}\right) \quad (10)$$

where μ is the dynamic viscosity in Pa·s.

Experimental results have shown that f always takes a value between 0.007 and 0.1, however its dependence on the Reynolds number is somewhat complex[29], and also depends on the pipe roughness.

4.1. Flow regimes

It is helpful to visualise the flow of fluids through pipes with the Moody diagram, see Figure 3. This relates the friction factor f against the Reynolds number Re and the pipe roughness ϵ/D, where ϵ is the absolute pipe roughness in m and D is the diameter of the pipe in m. This shows three regimes with different flow behaviour.
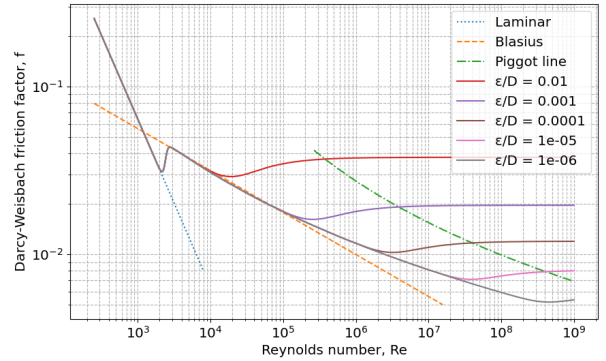

Figure 3: Moody diagram showing the friction factor as a function of the Reynolds number. The Piggot line marks the transition between inflectional- and fully-turbulent behaviour[31]. We use a modified Afzal equation[32] for the lines of different roughness as this is algebraically the most convenient of several which match the inflectional nikuradse behaviour[29, 33]

1. At the left-hand side of the Moody diagram is the laminar regime, which follows the analytical result of the Hagen-Poiseuille equation regardless of the roughness of the pipe (dotted line).
2. In the middle, between the laminar line (dotted) and the Piggot line (dash-dotted) there is the partially-turbulent regime. Most real gas distribution pipes operate in this regime.
3. At the right-hand side is the fully-turbulent regime, in which the friction factor depends only on roughness, and is independent of Re (horizontal lines to the right of the Piggot line).

Figure 3 shows lines for pipes of different roughnesses[10] for relative roughness values of 10^{-2}, 10^{-3}, 10^{-4}, and 10^{-5}.

The minimum visible at Re $\approx$ 2,300 is where the flow transitions from laminar to turbulent[29].

4.2. Regimes in the distribution network

Distribution networks for natural gas[11] are designed to run in the turbulent regime at peak design flow, with gas

---

[9] Weymouth, Panhandle A, Panhandle B, Spitzglass, various 'power laws', Colebrook[29, 30]. Many of these are dimensionally inhomogeneous and use 'industry units' where conversion factors are embedded in the equation constants, or where the range of applicability is not at all obvious to the user.

[10] There are at least 50 different semi-empirical equations which approximate the implicit Colebrook equation but these are simply mathematical fits and ignore the fact that the Colebrook equation itself does not describe experimental data to better than ± 15% [29, 32, 30].

[11] Numerical evidence is from the Netherlands[9] as UK gas network data is now redacted by the regulator.

velocities in the range 8-12 m/s. A general guideline for all gas networks is that the gas velocity should be between 5 and 10 m/s and always less than 20 m/s to prevent erosive wear by dust particles[9, 34, 35, 36].

The pressure drop, about 40 mbar, in the domestic connection is low compared with the absolute pressure, about 1 bar; so the behaviour does not change significantly along the pipe.

The maximum Reynolds number expected within the transmission may be calculated from the natural gas properties, the maximum velocity of 20 m/s, and the maximum pipe diameter of 630 mm[37]. This is a value of $Re = 1.0 \times 10^6$, which is in the middle of the partially-turbulent regime, as per Figure 3.

At the other end of the scale is the domestic connection, which in the UK is typically a 35 mm tube of drawn copper, steel, or polyethylene[1]. A typical domestic boiler in the UK is rated at 30 kW[28, 38]. The energy supply equation (4), as well as the material properties used in Section 3.7, allows us to calculate that the gas velocity of natural gas in this situation is v=0.838 m/s, and the Reynolds number is Re=2363. This places the flow at the lower end of the partially-turbulent regime.

Replacing natural gas with hydrogen in any piping system will always reduce the Reynolds number, because while the velocity increases, the density decreases significantly more, and the dynamic viscosity of also decreases[12]. See Section 4.7 for these calculations.

Calculating the Reynolds number for the domestic connection with pure hydrogen gives a value of at 970, quite definitely in the laminar flow regime where the pressure drop is linear in velocity. Therefore we need to consider multiple regimes that are applicable to different sections of the distribution network.

4.3. Partially-turbulent flow

The partially-turbulent regime in Figure 3 is between the laminar flow line and the Piggot line[13]. It was first reported in the discussion published at the end of the original Moody paper[31]. Behaviour in the partially-turbulent regime in Figure 3 may be further subdivided:

- The transition from laminar to turbulent flow, where the friction factor curve has a minimum[14].

- The Blasius sub-regime, shown as a dashed straight line.

---

[12]We use a simple molar fraction weighted approximation for the viscosity of gas mixtures, as that is adequate for the purpose of this paper. For modelling higher pressure transmission networks, a much more complex Chapman-Enskog or corresponding states[18] model would be required.

[13]Piggot observed this relationship between Re and relative roughness (ϵ/D) which is the point at which fully turbulent flow develops.

[14]This dependence is a characteristic of the physics of critical systems as shown by Goldenfeld[33].

	Density [kg/m³]	Dynamic viscosity [μPa·s]
H_2	0.0914	8.509
NG	0.0836	10.374
ratio	0.1902	0.8202

Table 5: Densities and dynamic viscosities at 8°C and 40 mbar

- The departure from the Blasius line, but where the friction factor continues to vary with Re, before the Piggot line is reached.

For Re less than 2×10^5 the friction factor follows the Blasius law, for more than 2×10^5 it diverges [29] but still depends on Re until the Piggot line. The friction factor f in the Blasius sub-regime is given by equation (9)[39].

$$f_{Blas} = 0.079 \times Re^{-1/4} \qquad (11)$$

For smooth pipes, such as steel or polyethylene with a relative roughness of 10^{-5}, the friction factor f for gas in distribution pipes varies between 0.008 and 0.045, as can be seen from Figure 3.

4.4. Pressure drop in the Blasius sub-regime

In the range of $Re \in (2 \times 10^3, 2 \times 10^5)$, we can combine the Darcy-Weisbach equation (9), the Blasius equation (11), and the Reynolds number definition (10), to give the dependence of pressure drop on all relevant parameters:

$$\Delta P = \left(\frac{4 \cdot 0.079}{D^{5/4}} \right) \cdot \rho^{3/4} \cdot \mu^{1/4} \cdot v^{7/4} \qquad (12)$$

In equation (12) the terms in brackets are constant when comparing any fluids in the same pipe. The remaining terms show the dependency on the properties, given in table 5, and the gas velocity. The material parameter $\rho^{3/4} \times \mu^{1/4}$ is almost independent of temperature[15].

Using equation (12) for the two fuels gives equation (13).

$$\left(\frac{\Delta P_{H_2}}{\Delta P_{NG}} \right)_{Blasius} = \left(\frac{\rho_{H_2}}{\rho_{NG}} \right)^{3/4} \left(\frac{\mu_{H_2}}{\mu_{NG}} \right)^{1/4} \left(\frac{v_{H_2}}{v_{NG}} \right)^{7/4}$$
$$(13)$$

Unlike equation (5) for the velocity ratio, equation (13) directly includes the density, ρ, as it is an important factor in the inertial forces giving rise to pressure drop. Using the material properties from table 5 and the velocity ratio from Section 3.7 for hydrogen and natural gas, we find the ratio of pressure drops of the two gases to be:

$$\left(\frac{\Delta P_{H_2}}{\Delta P_{NG}} \right) = 0.1902^{3/4} \times 0.8202^{1/4} \times 3.076^{7/4} = \mathbf{1.294}$$
$$(14)$$

---

[15] Varying by less than ± 1.2% over the range -40°C to +50°C, see Appendix D.1.

Now we can perform the iterative calculations to work out the average pipe pressure that was used in Section 3.5. The distribution network is controlled such that the low pressure end, P_{min}, is maintained at 20 mbar[1], and we have been using an average pressure for natural gas of $P_{av,NG} = 40$ mbar[16]. The average pipeline pressure is related to the minimum pressure and the pressure drop by:

$$P_{av} = \tfrac{1}{2}(P_{min} + P_{max}) = P_{min} + \tfrac{1}{2}\Delta P \qquad (15)$$

This may be combined for both hydrogen and natural gas to calculate the average pressure for hydrogen:

$$P_{av,H_2} = P_{min} + (P_{av,NG} - P_{min})\left(\frac{\Delta P_{H_2}}{\Delta P_{NG}}\right) \qquad (16)$$

Thus the iterative process is:

1. Make an initial guess for the value of P_{av,H_2}
2. Use this pressure in equation (5).
3. Use this velocity ratio in equation (13).
4. Use this pressure drop ratio in equation (16).
5. repeat steps 2 to 4 until the value of P_{av,H_2} converges.

The converged value is $P_{av,H_2} = 45.88$ mbar, which is the value that was used in Section 3.5 to be representative of a typical high-flow situation. This gives a maximum pressure within the pipe of 71.75 mbar, which is close to but below the maximum rating of 75 mbar[1].

4.5. Laminar regime

Below a Reynolds number of 2×10^3, all pipes regardless of roughness should exhibit laminar behaviour. The friction factor in this regime can be derived analytically from Poiseuille flow as:

$$f_{Lam} = \frac{64}{Re} \qquad (17)$$

This may be used in place of equation (11) for expressions for the pressure drop ratio and the compressor power ratio in the laminar regime with different exponents on the 3 terms:

$$\left(\frac{\Delta P_{H_2}}{\Delta P_{NG}}\right)_{Lam} = \left(\frac{\rho_{H_2}}{\rho_{NG}}\right)^0 \left(\frac{\mu_{H_2}}{\mu_{NG}}\right)^1 \left(\frac{v_{H_2}}{v_{NG}}\right)^1 = \mathbf{2.537} \qquad (18)$$

This value was calculated using the iterative method of section 4.4, in the limit that flow is slow enough that $\Delta P \ll P_{min}$, as we have no reasonable estimate of average pressure in a laminar slow situation. The corresponding velocity ratio in the laminar regime is 3.094.

4.6. Fully turbulent regime

At sufficiently high Reynolds number, flow enters the fully turbulent regime where f is independent of Re. For smooth drawn tubing with $(\epsilon/D) = 5 \cdot 10^{-5}$ this transition is at $Re = 3.5 \cdot 10^8$, determined by the Piggot relationship in equation (19).

$$\frac{3500}{\epsilon/D} = Re \qquad (19)$$

As the maximum obtainable Reynolds number in the distribution network is 10^6 from section 4.2, there is no way to achieve the fully turbulent regime without exceeding at least one of the network's design limitations.

4.7. General relationships

While the values derived above work well for cases in which the fluid regime is well defined, there are gaps between these regimes. The transition from laminar to partially turbulent behaviour is notoriously complex, however recent works have made an effort to understand this transition on a fundamental level[33, 30]. There is also a wide section of the partially-turbulent regime from $Re = 2 \times 10^5$ to 3.5×10^8 where the friction factor is not yet constant but also does not follow the Blasius equation. We hypothesise that much of the UK gas grid should be in this non-Blasius sub-regime.

Replacing natural gas with hydrogen can change the flow regime entirely. In the service pipe modelled in section 4.2, the regime was partially turbulent with natural gas, yet switching to hydrogen resulted in laminar flow.

For the gas velocity change of approximately $3\times$ from natural gas to hydrogen, depending on regime, there is a Reynolds' number shift which depends on the relative velocity changes and also on the relative densities of hydrogen and natural gas:

$$\left(\frac{Re_{H_2}}{Re_{NG}}\right) = \frac{\left(\frac{\rho_{H_2}}{\rho_{NG}}\right)\left(\frac{v_{H_2}}{v_{NG}}\right)}{\left(\frac{\mu_{H_2}}{\mu_{NG}}\right)} \qquad (20)$$

Using the modified Afzal equation for the friction factor, the increase in pressure drop may be plotted against the any pipeline Reynolds number for natural gas in Figure 4. The Reynolds number for hydrogen will be less than the x-axis value by equation (20), for the same pipe geometry, and this has been incorporated into the calculations.

Figure 4 shows that at locations and times where the natural gas flow is slower, there will be a proportionally larger increase in the pressure drop by switching to hydrogen. The dip at $Re \approx 5 \times 10^3$ is where the switch to hydrogen causes the flow to change from turbulent to laminar, which can result in a decrease in the pressure drop in the pipe. The transition is effectively a time-average of an unstable switching between these two states, but it is not practical to design systems to make use of this.

The increase in the compression power for hydrogen over natural gas has been noted by Schouten[9] and others,
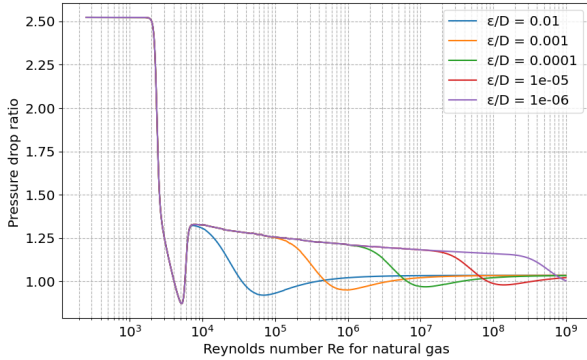
Figure 4: The increase in pressure drop as a function of the Reynolds number for natural gas, when replacing natural gas with hydrogen. The curves for the friction factor and compressor power follow the same trend, but are scaled by combinations of the ratios of density, viscosity, and velocity, which are independent of the Reynolds number. These curves make use of the assumption of incompressible flow, so should be treated with caution for gases at very high Reynolds numbers.

but only for fully-turbulent conditions. The increase in friction factor and the consequent increase in compressor power required has not previously been recognised.

4.8. Pumping power

The pressure drop of a flowing fluid arises from frictional losses. The pumping power, W, required to overcome these losses for an incompressible fluid is the product of the pressure drop and the volumetric flow rate. In a pipe[39] this is:

$$W = \Delta P \cdot v \cdot A \tag{21}$$

The proportional increase in the compression power requirement when switching from natural gas to hydrogen is therefore the ratio of this equation for the two gases:

$$\left(\frac{W_{H_2}}{W_{NG}} \right) = \left(\frac{\Delta P_{H_2}}{\Delta P_{NG}} \right) \left(\frac{v_{H_2}}{v_{NG}} \right) \tag{22}$$

As we have shown, the velocity ratio is largely independent of the flow regime and depends mostly on the thermodynamics of combustion, this means that the ratio of compressor power follows the exact same trend as the ratio of pressure drop does in Figure 4, with the values all scaled up by the velocity ratio, 3.076.

We can calculate individual values for the two major regimes. In the Laminar regime $(W_{H_2}/W_{NG})Lam = 7.76$, and in the Blasius regime where we expect the majority of the distribution network to operate, $(WH_2/W_{NG})_{Blas} = 3.98$. Even in the dip where the pressure ratio is less than one, the compressor power still increases by approximately $2.5\times$ due to the much faster gas velocity for hydrogen.

Since we expect most of the flow in the distribution network to be in the Blasius regime, this tells us that the energy required to deliver hydrogen through the distribution network will be $3.98\times$ greater than for natural gas.

5. UK distribution capabilities

Much of the older network runs at only 50 mbar [3] to reduce leakage, where this still gives adequate pressure (20 mbar) at the most distant user. This could be increased up towards the maximum 75 mbar level with new polyethylene pipe which is less prone to leaks[3].

The UK domestic gas demand[40] peaked in 2004 at 34,035 toe[16] and in the most recent cold winter year (2021) it was 26,275 toe. This means that the network today can cope with an annual demand of natural gas at least 29.5% higher than it currently supplies. While it is possible that during the peak hourly demands of 2004 and 2021 this ratio was less than the annual ratio, we can only expect that this over-capacity will continue to grow into the future as more houses get insulated, upgraded or replaced and also due to climate change reducing the heating demand overall[41].

6. Conclusions

While it is clear that burning hydrogen for heat in a boiler, or even in a combined heat and power cell, is almost a use of last resort[42, 43], there appear to be no pressure difficulties with delivering pure hydrogen using the existing UK distribution network. This paper shows that the velocity is similar to that which had previously been thought but that the pressure drop and power requirement are higher.

It has not previously been noted that:

- Burning hydrogen means that care must be taken to reduce the condensation temperature of the condensing boiler as much as possible because a greater proportion of the combustion energy is in the form of condensible water.

- Using hydrogen reduces the Reynolds' number of the flow rather than increasing it.

- There is a slight effect of increasing the mean pressure, and thus the energy density, of the hydrogen because it requires a 29% higher pressure gradient to be delivered.

- The Blasius material parameter $\rho^{3/4} \cdot \mu^{1/4}$ has a very low temperature dependence, meaning that our conclusions on relative pressure drop and the relative compression power are largely insensitive to temperature whilst the Blasius equation holds.

- As well as the low pressure system investigated here in detail, we hypothesise that the Medium and Intermediate Pressure distribution pipes are operating for much of the time in the partially-turbulent regime.

---

[16]toe = tonne of oil equivalent, 1 toe is equal to 11.63 MWh

7. References

[1] P. Dodds, S. Demoullin, Conversion of the uk gas system to transport hydrogen, International Journal of Hydrogen Energy 38 (18) (2013) 7189–7200.
URL http://dx.doi.org/10.1016/j.ijhydene.2013.03.070

[2] Royal Academy of Engineering, Centre National Engineering Policy, The role of hydrogen in a net zero energy system, Tech. Rep. September, Royal Academy of Engineering (2022).
URL https://raeng.org.uk/media/tkphxfwy/the-role-of-hydrogen-in-the-net-zero-energy-system.pdf

[3] ARUP, Future of great britain's gas networks - final report for national infrastructure commission and ofgem (2023).
URL https://nic.org.uk/app/uploads/Arup-Future-of-UK-Gas-Networks-18-October-2023.pdf

[4] NationalGrid, Hydrogen blends in the nts - a theoretical exploration gas future operability planning (2021).
URL https://www.nationalgas.com/document/137506/download

[5] NationalGas, Gas ten year statement network capability (2023).
URL https://www.nationalgas.com/insight-and-innovation/gas-ten-year-statement-gtys

[6] S. Samsatli, N. J. Samsatli, The role of renewable hydrogen and inter-seasonal storage in decarbonising heat comprehensive optimisation of future renewable energy value chains, Applied Energy 233-234 (2019) 854–893. doi:10.1016/j.apenergy.2018.09.159.

[7] U. Bossel, Does a hydrogen economy make sense?, Proceedings of the IEEE 94 (10) (2006) 1826–1836. doi:10.1109/JPROC.2006.883715.
URL https://www.researchgate.net/publication/2998127_Does_a_Hydrogen_Economy_Make_Sense

[8] O. S. Ibrahim, A. Singlitico, R. Proskovics, S. McDonagh, C. Desmond, J. D. Murphy, Dedicated large-scale floating offshore wind to hydrogen: Assessing design variables in proposed typologies, Renewable and Sustainable Energy Reviews 160 (March) (2022) 112310. doi:10.1016/j.rser.2022.112310.
URL https://doi.org/10.1016/j.rser.2022.112310

[9] J. A. Schouten, J. P. J. Michels, R. J. van Rosmalen, Effect of h2-injection on the thermodynamic and transportation properties of natural gas, International Journal of Hydrogen Energy 29 (2004) 1173–1180.
URL https://www.sciencedirect.com/science/article/abs/pii/S0360319903003112

[10] A. Witkowski, A. Rusin, M. Majkut, K. Stolecka, Analysis of compression and transport of the methane/hydrogen mixture in existing natural gas pipelines, International Journal of Pressure Vessels and Piping 166 (2018) 24–34. doi:10.1016/j.ijpvp.2018.08.002.
URL https://www.sciencedirect.com/science/article/pii/S0308016118301698

[11] K. Altfeld, D. Pinchbeck, Admissible hydrogen concentrations in natural gas systems (2013).
URL www.gas-for-energy.comhttps://www.gerg.eu/wp-content/uploads/2019/10/HIPS_Final-Report.pdf

[12] M. Witek, F. Uilhoorn, Impact of hydrogen blended natural gas on linepack energy for existing high pressure pipelines, Archives of Thermodynamics 43 (2022) 111–124. doi:10.24425/ather.2022.143174.

[13] cngservices, Fordoun case study (2019).
URL https://www.cngservices.co.uk/case_study/fordoun/

[14] P. Sargent, M. Sargent, Hydrogen in pipes - software (Dec. 2023). doi:10.5281/zenodo.10368611.
URL https://github.com/PhilipSargent/h2-in-pipes

[15] D. J. C. MacKay, Sustainable Energy - Without the Hot Air, UIT Cambridge Ltd., 2008, Ch. E Heating II, pp. 303–304.
URL https://www.withouthotair.com/cE/page_303.shtml

[16] UTONOMY, Utonomys pressure management (2023).
URL https://bit.ly/utonomy

[17] M. L. Huber, E. W. Lemmon, I. H. Bell, M. O. McLinden, The nist refprop database for highly accurate properties of industrially important fluids (10 2022). doi:10.1021/acs.iecr.2c01427.
URL https://webbook.nist.gov/cgi/cbook.cgi

[18] I. H. Bell, J. Wronski, S. Quoilin, V. Lemort, Pure and pseudo-pure fluid thermophysical property evaluation and the open-source thermophysical property library coolprop, Industrial & Engineering Chemistry Research 53 (6) (2014) 2498–2508. arXiv:http://pubs.acs.org/doi/pdf/10.1021/ie4033999, doi:10.1021/ie4033999.
URL http://pubs.acs.org/doi/abs/10.1021/ie4033999

[19] S. 284, The gas safety (management) (amendment) regulations 2023 (3 2023).

[20] D. R. Burgess, A. P. Hamins, Technical Note Heats of Combustion and Related Properties of Pure Substances Heats of Combustion and Related Properties of Pure Substances, NIST, 2023.

[21] H. Satyavada, S. Baldi, Monitoring energy efficiency of condensing boilers via hybrid first-principle modelling and estimation, Energy 142 (2018) 121–129. doi:10.1016/j.energy.2017.09.124.

[22] Cleaver-Books, The impact of excess air on efficiency (9 2016).
URL https://www.watmfg.com/watmfg23082016/wp-content/uploads/2016/09/Excess-Air-and-Boiler-Efficiency.pdf

[23] Y. Zhao, H. Diao, Y. Qin, L. Xie, M. Ge, Y. Wang, S. Wang, Effect of flow rate on condensation of CO2-water vapor mixture on a vertical flat plate, Applied Thermal Engineering 229 (2023) 120557. doi:https://doi.org/10.1016/j.applthermaleng.2023.120557.
URL https://www.sciencedirect.com/science/article/pii/S1359431123005860

[24] R. H. Perry, D. W. Green, J. O. Maloney, Perry's Chemical Engineers' Handbook, 8th Edition, McGraw-Hill, 2008.
URL https://api.semanticscholar.org/CorpusID:56182942

[25] BEIS, Review of the methodology for fghrs in sap final report (2021).
URL https://assets.publishing.service.gov.uk/media/614b218ee90e077a2db2e793/review-methodology-fghrs-sap.pdf

[26] DESNZ, Lab testing - boiler cycling (12 2023).
URL https://assets.publishing.service.gov.uk/media/65785a000467eb000d55f5ce/hem-val-05-lab-testing-boiler-cycling.pdf

[27] N. Terry, R. Galvin, How do heat demand and energy consumption change when households transition from gas boilers to heat pumps in the UK, Energy and Buildings 292 (2023) 113183. doi:10.1016/j.enbuild.2023.113183.
URL https://linkinghub.elsevier.com/retrieve/pii/S0378778823004139

[28] G. Orr, T. Lelyveld, BurtonSimon, Final report: In-situ monitoring of efficiencies of condensing boilers and use of secondary heating (6 2009).
URL https://assets.publishing.service.gov.uk/media/5a75149be5274a3cb28697f7/In-situ_monitoring_of_condensing_boilers_final_report.pdf

[29] J. J. Allen, M. A. Shockling, G. J. Kunkel, A. J. Smits, Turbulent flow in smooth and rough pipes, Philosophical Transactions of the Royal Society A: Mathematical, Physical and Engineering Sciences 365 (1852) (2007) 699–714. doi:10.1098/rsta.2006.1939.

[30] Z. S. She, Y. Wu, X. Chen, F. Hussain, A multi-state description of roughness effects in turbulent pipe flow, New Journal of Physics 14. doi:10.1088/1367-2630/14/9/093054.

[31] L. Moody, Friction factors for pipe flow, Transactions of the ASME 66 (1944) 671–684.

[32] R. T. Cerbus, C. C. Liu, G. Gioia, P. Chakraborty, Laws of Resistance in Transitional Pipe Flows, Physical Review Letters 120 (5) (2018) 54502. doi:10.1103/PhysRevLett.120.054502.
URL https://doi.org/10.1103/PhysRevLett.120.054502

[33] N. Goldenfeld, Roughness-induced critical phenomena in a tur-

bulent flow, Physical Review Letters 96 (4) (2006) 1–4. arXiv: 0509439, doi:10.1103/PhysRevLett.96.044503.

[34] F. Tabkhi, C. AzzaroPantel, L. Pibouleau, S. Domenech, A mathematical framework for modelling and evaluating natural gas pipeline networks under hydrogen injection, International Journal of Hydrogen Energy 33 (2008) 6222–6231.
URL https://www.sciencedirect.com/science/article/abs/pii/S0360319908009634

[35] E. K. Ejomarie, E. G. Saturday, Optimal design of gas pipeline transmission network, Global Scientific Journals 8 (2020) 918–933.
URL www.globalscientificjournal.com

[36] A. J. Abbas, H. Hassani, M. Burby, I. J. John, An Investigation into the Volumetric Flow Rate Requirement of Hydrogen Transportation in Existing Natural Gas Pipelines and Its Safety Implications, Gases 1 (4) (2021) 156–179. doi:10.3390/gases1040013.

[37] GPS, GPS PE Pipe Systems Installation and Technical Guidelines, Tech. rep., GPS PE Pipe Systems Ltd. (2008).
URL https://web.archive.org/web/20130319072835/http://www.bssindustrial.co.uk:80/uploads/docs/698.pdf

[38] G. Bennett, C. Elwell, Effect of boiler oversizing on efficiency: a dynamic simulation study, Building Services Engineering Research and Technology 41 (6) (2020) 709–726. doi:10.1177/0143624420927352.

[39] C. A. Bennett, R. P. Hohmann, Methods for calculating shear stress at the wall for single-phase flow in tubular, annular, plate, and shell-side heat exchanger geometries, Heat Transfer Engineering 38 (2017) 829–840. doi:10.1080/01457632.2016.1211913.
URL https://doi.org/10.1080/01457632.2016.1211913

[40] DESNZ, Ecuk 2023: End uses data tables (excel) (9 2023).
URL https://www.gov.uk/government/statistics/energy-consumption-in-the-uk-2023

[41] N. Christidis, M. McCarthy, P. A. Stott, Recent decreases in domestic energy consumption in the united kingdom attributed to human influence on the climate, Atmospheric Science Letters 22. doi:10.1002/asl.1062.

[42] J. Rosenow, A meta-review of 54 studies on hydrogen heating, Cell Reports Sustainability (2023) 100010doi:10.1016/j.crsus.2023.100010.

[43] M. Liebreich, The clean hydrogen ladder [now updated to v4.1] - liebreich (8 2021).
URL https://www.liebreich.com/the-clean-hydrogen-ladder-now-updated-to-v4-1/

[44] D. Lozano-Martn, A. Moreau, C. R. Chamorro, Thermophysical properties of hydrogen mixtures relevant for the development of the hydrogen economy: Review of available experimental data and thermodynamic models, Renewable Energy 198 (2022) 1398–1429. doi:10.1016/j.renene.2022.08.096.
URL https://www.sciencedirect.com/science/article/pii/S096014812201271X

[45] DLUHC, English housing survey 2021 to 2022: headline report (2022).
URL https://bit.ly/3Hf4qOv

[46] F. J. Krieger, Calculation of the Viscosity of Gas Mixtures, Tech. rep., RAND Corporation (1951).
URL https://www.rand.org/pubs/research_memoranda/RM649.html

[47] A. Pina-Martinez, R. Privat, J.-N. Jaubert, D.-Y. Peng, Updated versions of the generalized soave -function suitable for the redlich-kwong and peng-robinson equations of state, Fluid Phase Equilibria 485 (2019) 264–269. doi:10.1016/j.fluid.2018.12.007.

[48] R. Privat, J. N. Jaubert, The state of the art of cubic equations of state with temperature-dependent binary interaction coefficients: From correlation to prediction, Fluid Phase Equilibria 567. doi:10.1016/j.fluid.2022.113697.

Acknowledgements

Appendix A. Software used in this study

The python code and input data is published on GitHub: https://github.com/PhilipSargent/h2-in-pipes under the MIT open source license[14].

Appendix B. Compressibility

All calculations in this paper have used an equation of state and mixing rules appropriate to the pressure and temperature for each pure gas or blend studied. Individual corrections are small, but they multiply together to make a significant difference.

To calculate the compression factor as a function of temperature and pressure, and for gases such as natural gas composed of several different compounds, one needs an equation of state. The low pressures and ambient temperatures of the distribution grid mean that several different equations of state are all sufficiently accurate.

Lozana *et al.* have recently reviewed[44] the relevant equations of state and there are a bewildering variety of suitable functions.

In this paper we use the 1978 Peng-Robinson equation of state[34, 36], with temperature dependent binary interaction parameters and no volume translation corrections. For the exact calculation method used in this paper, see the code[14].

Appendix C. Upgrading UK Boilers

In the most recent English housing survey[45], approximately one tenth $(7/(59+7))$ of domestic boilers on piped-gas were non-condensing and nine-tenths condensing: "the proportion of dwellings with a standard boiler decreased from 9% in 2020 to 7% in 2021, while the proportion with a condensing-combination boiler has increased from 57% to 59% in the same period".

However there are no statistics on how many of the condensing boilers have correctly-adjusted 50°C return-flow settings with appropriate weather compensation. Anecdotally, the proportion is very small, very likely less than 5%. So a reasonable estimate would be that the return temperature is set to 50°C for 5% of the condensing boilers and to 70°C for 95% of them. There is no condensing for the non-condensing boilers so their efficiency is simply that at a 'condensation' temperature of 100°C.

We will assume

- That 4% of boilers are already perfectly adjusted, and the only change will be the multiplier of 0.974× from the change in fuel condensation behaviour

- That 86% of boilers will go from a condensing temperature of 70°C (87.44% with NG) to 50°C (93.69% with hydrogen), a multiplier of 0.933×

- That 10% of boilers will change from an efficiency of 86.20% (non condensing) to a fully-condensing, properly adjusted reflow temperature of 50°C (93.69% with hydrogen), a multiplier of 0.920×

The population weighted efficiency multiplier is thus 0.933×.

Appendix C.1. Published boiler efficiencies

Boiler efficiency[39] is measured either in a test rig at steady-state load, or estimated as a seasonal average as-installed in a house with a typical daily heating cycle and weather pattern. Repeated on- and off-periods increase losses[21]. Boiler manufacturer published efficiency values may be legally-required in some jurisdictions to be a seasonally-adjusted average number.

Appendix D. Viscosities and temperature

The viscosities of pure components are calculated from experimental data as a least-squares fit to a power law dependence on absolute temperature. Ideal gases have a power law relationship where the exponent is 0.5, the real gases here have exponents between 0.66 and 1.08. The viscosity of the gas mixture is a molecular fraction weighted average[46] of the viscosities of the components.
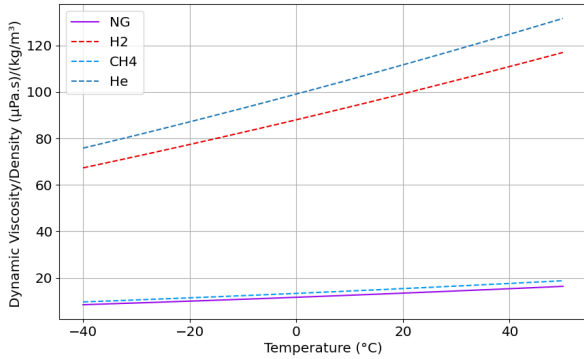

Figure D.5: Plot of kinematic viscosity: the ratio of dynamic viscosity and density, as a function of temperature at 1.06825 bar

Figure D.5 shows the temperature dependence of the kinematic viscosities (the ratio of density to dynamic viscosity) of the natural gas blend, hydrogen and methane. This shows why it is important to do these calculations at a well-chosen reference temperature rather than using textbook values which may have been measured at a variety of different temperatures.

In the UK the ground temperature of the buried LP network is likely to stay in the range 5 to 15°C all year[15].

Appendix D.1. The Blasius materials property

Note that the term $\rho^{3/4} \cdot \mu^{1/4}$ in equation (12) is a materials' property which depends on temperature and pressure. We define this property as B, the Darcy-Weisbach Reynolds-Blasius parameter in equation (D.1); or abbreviated to the 'Blasius parameter'.
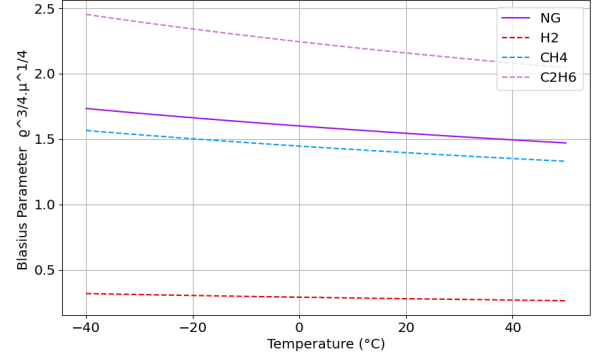

Figure D.6: Blasius Parameter $\rho^{3/4} \cdot \mu^{1/4}$ $((kg/m)\cdot(m\cdot s)^{-4}$)

$$B = \rho^{3/4} \cdot \mu^{1/4} \tag{D.1}$$

where ρ is the density and μ is the dynamic viscosity.

Somewhat surprisingly, this materials' property has only a slight dependence on temperature as the dependencies of density and viscosity act in opposite directions.

Also surprisingly, all the gases in the study have very similar dependence such that the normalised Blasius parameter, where the value for each gas is divided by the value for natural gas, is very nearly independent of temperature, varying less than 1.2% between -40°C and +50°C.

This means that results calculated using the Blasius parameter, the relative pressure drop and the relative compression power requirement, are independent of temperature in the distribution grid.

Appendix E. Dew point and partial pressure

Our calculations produce the partial pressure of water vapour in the flue gas, but we need the dew point. The two are related by standard tables of the saturation vapour pressure of water[24]: the pressure at which water vapour is in thermodynamic equilibrium with its condensed state.

The range of atmospheric pressure in the UK means that the dew point of the flue gas varies ±1.4°C, which affects the maximum efficiency.

Appendix F. The Peng-Robinson calculations

Equations of state for gas mixtures are still an active research area[44] and there is continual development of alpha functions, interaction parameters and mixing rules e.g. Pina-Martinez *et al.*[47].

Appendix F.1. Calculating the properties of a gas mixture

The higher heat capacity and the mean molecular weight of the Fordoun natural gas are calculated from a mole fraction weighted sum of those properties of the component pure gases.

The compressibility and density of the natural gas are calculated for a given temperature and pressure using the Peng-Robinson equation of state:

1. The Peng-Robinson[47] parameters a (attraction) and b (repulsion) for each pure component at a given temperature are calculated from the critical temperature T_c, the critical pressure P_c, and the *omega* coefficient (a measure of the molecule asphericity) of each pure gas.

2. the coefficient b of the mix is the weighted sum of the b values of the component gases, where the weights are the mole fractions.

3. The temperature dependent binary interaction parameter k is calculated using the Courtinho method [48] from the b value of each gas in a pair. For an 11 component gas there are 55 pairwise interactions.

4. The a values are calculated as the weighted sums of the geometric means of the pair-wise values of a between each pair of components. The weights are the mole factions of each pair multiplied together, times the value (1-k)

5. The effective T_c, P_c and *omega* of the natural gas, the pseudo-component, are calculated from the a and b values for the mix for the given temperature

6. the compressibility and thus the density of the natural gas is calculated using the effective T_c, P_c and *omega* values.

The precise algorithm is in the code on GitHub [14].